

The Maximums of the Seebeck Coefficient and Figure of Merit of Thermoelectric

Zurab Adamia, George Kakhniashvili, Revaz Kokhreidze and Nakhutsrishvili Irakli*

Georgian Technical University, 0186 Tbilisi.

Corresponding Author: Nakhutsrishvili Irakli, Georgian Technical University, 0186 Tbilisi.

Received: 2024 Dec 25

Accepted: 2025 Jan 14

Published: 2025 Jan 25

Abstract

This article provides an assessment of the maximum values of the most important thermoelectric parameters of materials - the Seebeck coefficient and the figure of merit. Based on the formulas known from the literature that interconnect the thermoelectric parameters (effective mass and mobility of charge carriers, the Seebeck coefficient, temperature), the function of the specified coefficient is obtained. To estimate the maximum of the Seebeck coefficient and the figure of merit, it is sufficient to study this function for an extremum by differentiating it be used. The data we obtained can be used to analyze the experimental data of those works in which, for certain reasons, the extremums of the specified thermoelectric parameters are not given.

Keywords: Thermoelectric, Seebeck Coefficient, Figure of Merit

1. Introduction

The Seebeck effect is that if the ends of a metal or semiconductor sample are at different temperatures, thermal diffusion will occur. Since the thermal motion of electrons at the hot end is faster than at the cold end, more electrons will move from the hot end to the cold end than in the opposite direction. The current resulting from this diffusion causes the cold end to become negatively charged relative to the hot end, causing a voltage to develop between the two ends. The thermal diffusion voltage U is proportional to the temperature difference between the two ends (T_1 - temperature at the hot end, T_2 - temperature at the cold end): $U = S(T_1 - T_2)$, where the proportionality coefficient S is called the Seebeck coefficient. The Seebeck effect is used in voltage and temperature sensors, gas pressure meters, thermal electric generators, light intensity controllers and in many other equipments. They are used in navigation systems, generators, spacecraft, solar energy converters, heating equipment, oil and gas processing plants, thermal energy converters. The Seebeck coefficient often has extreme values, in many cases - both minimum and maximum [1-31]. This is demonstrated in Figs (1-3) based on literary and our data.

The data on $\text{Bi}_2\text{S}_3-x\text{Te}_x$ and $\text{Cr}_x\text{Mo}_{1-x}$ were taken from the literature we studied the alloy SixGe_{1-x} . The studied samples were produced by vacuum hot pressing of powders obtained from zone melting ingots [5,6].

In this paper, the extremums of the Seebeck coefficient and figure of merit are considered. For practical purposes, it is of interest to determine the maximums of these this characteristic.

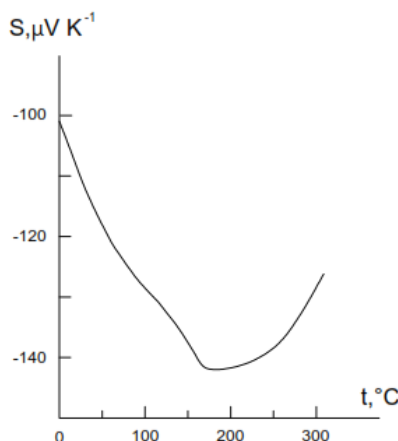


Figure 1: S – T Dependence for $\text{Bi}_2\text{S}_{3-x}\text{Te}_x$ from [5]; (the Value of x is Notspecified)

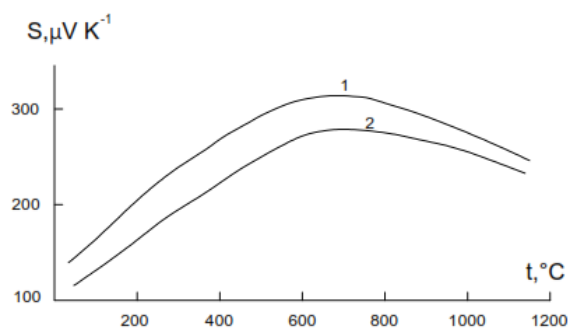


Figure 2: S - T Dependence for $\text{Si}_x \text{Ge}_{1-x}$: $x=0.3$ (1) and 0.17 (2)

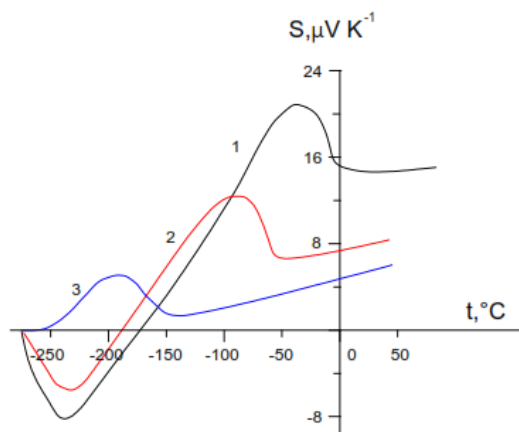


Figure 3: S - T Dependence for $\text{Cr}_x \text{Mo}_{1-x}$ from [6]: $x=0.03$ (1), 0.07 (2) and 0.15 (3)

1.1. Experimental

The composition of alloys significantly impacts their mechanical properties. For instance, the addition of alloying elements can alter strength, ductility, and corrosion resistance. In additive manufacturing, the choice of alloy is crucial as it determines how the material responds to the thermal cycles of the process. Techniques such as heat treatments and hot isostatic pressing can enhance the mechanical properties by reducing residual stresses, improving microstructure, and eliminating defects. The build environment, including temperature and atmospheric conditions, can influence oxidation and contamination, indirectly affecting mechanical properties. Controlling these conditions is crucial for ensuring the quality and performance of the alloys. Since the previous section mainly describes literature data, here we will describe only the procedure for preparing of SiGe samples.

To create a thermoelectric module, n- and p-type $\text{Si}_0.7\text{Ge}_0.3$ alloys containing alloying substances with a concentration of $3.2 \cdot 10^{26} \text{ m}^{-3}$ were fabricated by the vacuum hot-pressing method. Massive wastes of Si and Ge were crushed with a steel rod and sieved through a (with 0.2 mm cells) sieve. Then it was loaded into the mill chamber ("REC" PM-100 SM) and ground for 20-25 hours. The powder grain size was assessed using an optical microscope (Nikon) and an X-ray diffractometer (DRON-3M). The dispersed $\text{Si}_0.7\text{Ge}_0.3$ alloy powder produced in the indicated mode consisted mainly of Si and Ge grains of size 60–80 nm. The resulting powder was pressed in a high-temperature vacuum induction pressure chamber at a temperature of 1200-1320°C and a pressure of 480 kg·cm⁻² for 20-30 minutes. The matrix and punches are made of high-strength graphite. From the obtained briquettes, profiled samples were cut out on a diamond-cutting disk device. Photo of briquette is shown in Fig.4. Graphite switching plates were attached to the ends of the alloy branches. The switched sample was placed in the vacuum chamber of an induction furnace, and probes were placed in its switching plates to measure the temperature and electromotive force. One side of the module was heated by a flame generated by gas combustion, which directly hit the surface of the module. On the other side, the module was cooled by running water. Chromel-alumel thermocouples were placed on the hot and cold ends of the module. The monolithic thermoelectric module's cold side electrical insulation node was fabricated using AlN and graphite plates. Both of them are thermomechanically combined with SiGe alloys in a wide temperature range, which is very important for creating a thermostable. Figure 5 shows photo of module from 16 branches. 4 n- and p-type alloy plates (2 n-type and 2 p-type) were taken to make a mini monolithic thermoelectric module containing 16 branches. They were arranged in n-p-n-p order.



Figure 4: Photo of Briquette Compacted from Ultra Dispersed $\text{Si}_{0.7}\text{Ge}_{0.3}+\text{P}_{0.5}$ Alloy Powder at 1300°C

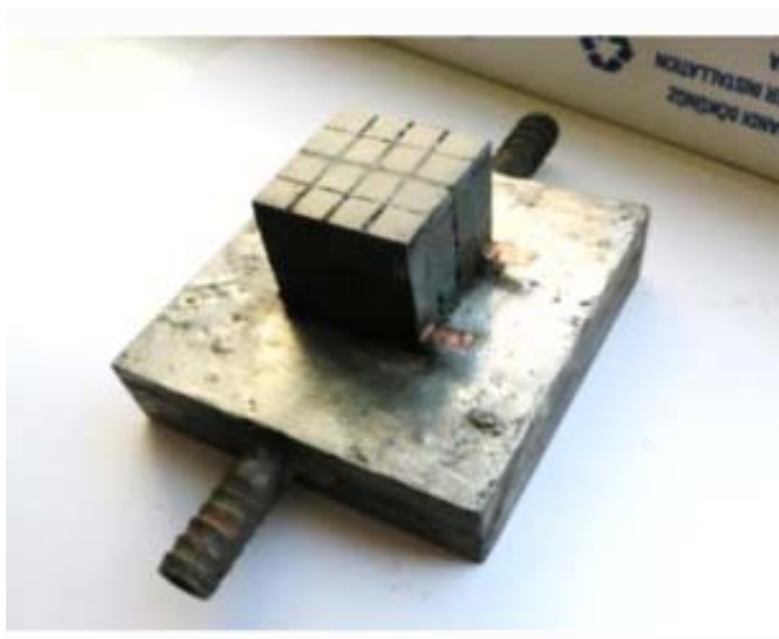


Figure 5: Photo of Thermoelectric Module Connected to Water Cooler

2. Results and Discussion

To compile an expression for S , formulas known from the literature (Snyder et al. 2022) relating the absolute temperature (T), effective mass (m^*), and concentration of charge carriers (n) are used

$$S \sim \frac{m^*T}{n^{2/3}}, \quad m^* \sim \left(\frac{n^{2/3}}{T}\right) \left\{ \frac{[e^{(S_T-2)} - 0.17]^{2/3}}{1 + e^{-5(S_T - S_T^{-1})}} + \frac{S_T}{1 + e^{5(S_T - S_T^{-1})}} \right\}, \quad S_T = \frac{q_e}{k_B} |S| \approx 11605 |S|$$

reduced Seebeck coefficient (q_e – elementary charge, k_B – Boltzmann's constant). By combining these formulas, we obtain the expression:

$$f(S) \sim \left\{ \frac{[e^{(11605|S|-2)} - 0.17]^{2/3}}{11605|S|[1 + e^{-5(11605|S|-8.617 \cdot 10^{-5}|S|^{-1})}]} + \frac{1}{1 + e^{5(11605|S|-8.617 \cdot 10^{-5}|S|^{-1})}} \right\}. \quad (1)$$

Figure 6 shows the dependence $f(S) - S$ and $f'(S) - S$, on which the extremes are clearly expressed.

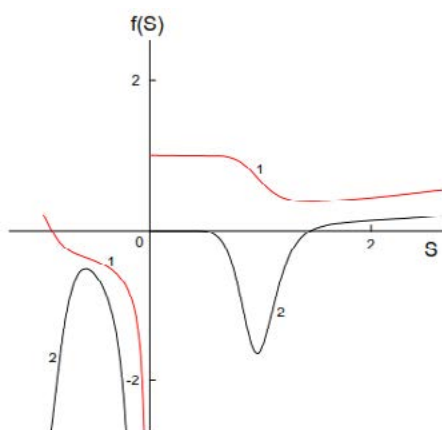


Figure: 6 Dependences $f(S) - S$ (1) and $f'(S)$ (2) According to Eq. (1)

After of this, it is easy to determine the maximum figure of merit $ZT = (\sigma S^2) T/k$, where σ is specific electrical conductivity and k is thermal conductivity coefficient (the sum of its electronic and lattice components). Using the Wiedemann-Franz law we will have $ZT \sim S^2$ and $(ZT)_{\max} \sim (S^2)_{\max} \sim S_{\max}$.

The presented approach can be used to predict the maximum values of the considered thermoelectric parameters in cases where they are not revealed due to the limitation of their measurement range.

3. Conclusion

The maximum values of thermoelectric parameters of materials - Seebeck coefficient and figure of merit are estimated. Based on the formulas known from the literature, which interconnect the thermoelectric parameters, the function of the mentioned coefficient is obtained. To estimate the maxima of the Seebeck coefficient and the figure of merit, it is sufficient to study this function for an extremum by differentiating it. The obtained data can be used to analyze the experimental data of those works in which, for some reason, the maxima of the specified thermoelectric parameters are not given.

The maximum values of thermoelectric parameters of materials - Seebeck coefficient and figure of merit are estimated. Based on the formulas known from the literature, which interconnect the thermoelectric parameters, the function of the mentioned coefficient is obtained. To estimate the maxima of the Seebeck coefficient and the figure of merit, it is sufficient to study this function for an extremum by differentiating it. The obtained data can be used to analyze the experimental data of those works in which, for some reason, the maxima of the specified thermoelectric parameters are not given.

Footnote:

Having estimated the maximum Seebeck coefficient, we can also consider the issue of maximization the power factor $PF \equiv \sigma S^2 = nq\mu S^2$ (μ - mobility of charge carriers). Using the equations from [27,28] we get:

$$\mu \cong \left(\frac{m^*}{m_0}\right)^{-3/2} \mu_W,$$

$$\frac{m^*}{m_0} \sim \left(\frac{n^{2/3}}{T}\right) \left\{ \frac{3[e^{(S_r-2)} - 0.17]^{2/3}}{1 + e^{-5(S_r - S_r^{-1})}} + \frac{S_r}{1 + e^{5(S_r - S_r^{-1})}} \right\},$$

$$\mu_W \sim \left\{ \frac{e^{(S_r-2)}}{1 + e^{-5(S_r-1)}} + \frac{\frac{3}{\pi^2} S_r}{1 + e^{5(S_r-1)}} \right\} \rightarrow$$

$$\rightarrow PF \sim T^{3/2} \left\{ \frac{[e^{(S_r-2)} - 0.17]^{2/3}}{1 + e^{-5(S_r - S_r^{-1})}} + \frac{S_r}{1 + e^{5(S_r - S_r^{-1})}} \right\} \left\{ \frac{e^{(S_r-2)}}{1 + e^{-5(S_r-1)}} + \frac{\frac{3}{\pi^2} S_r}{1 + e^{5(S_r-1)}} \right\} \left\{ \frac{3[e^{(S_r-2)} - 0.17]^{2/3}}{1 + e^{-5(S_r - S_r^{-1})}} + \frac{S_r}{1 + e^{5(S_r - S_r^{-1})}} \right\}^2,$$

where μ_W is weighted mobility [27,28].

To determine $(PF)_{\max}$, the function $f(T, m^*, \mu_W) = f(T, S)$ should be considered using the Lagrange multiplier method. This issue will be discussed in the continuation of this communication.

Acknowledgements

This article is dedicated to the memory of the director of the Sukhumi Institute of Physics and Technology Guram Bokuchava.

References

1. Ahmad, M., Agarwal, K., & Mehta, B. R. (2020). An anomalously high Seebeck coefficient and power factor in ultrathin Bi₂Te₃ film: Spin-orbit interaction. *Journal of Applied Physics*, 128(3).
2. Barbakadze, K., Bokuchava, G., Isakadze, L., et al. (2022). High temperature thermoelectric generator based on SiGe alloy. *LELP – Agmashenebeli National Defence Academy of Georgia*, 47-52.
3. Bhagade, S., Debnath, A., Das, D., & Saha, B. (2022). Thermoelectric composite material of CuBO₂ incorporated PANI powders with enhanced Seebeck coefficient. *Journal of Polymer Research*, 29(12), 505.
4. Bian, Z., Zebarjadi, M., Singh, R., Ezzahri, Y., Shakouri, A. et al. (2007). Cross-plane Seebeck coefficient and Lorenz number in superlattices. *Physical Review B—Condensed Matter and Materials Physics*, 76(20), 205311.
5. Cadavid, D., Ibáñez, M., Anselmi-Tamburini, U., Durá, O. J., Torre, M. A. L. D. L. et al. (2014). Thermoelectric properties of bottom-up assembled Bi₂S₃-x Te_x nanocomposites. *International journal of nanotechnology*, 11(9-1011), 773-784.
6. Muchono, B., Sheppard, C. J., Prinsloo, A. R. E., & Alberts, H. L. (2014). Magnetic susceptibility studies of the (Cr₉₈.4Al₁.6) 100-x Mox alloy System.
7. Chebbab, I., Chiker, F., Baki, N., Miloua, R., Khachai, Y. A. et al. (2024). An accurate DFT insights into optoelectronic, magnetic, thermodynamic and thermoelectric characteristics of monoclinic spiroffite Co₂Te₃O₈. *Optical and Quantum Electronics*, 56(8), 1299.
8. Craco, L., & Leoni, S. (2024). Effect of localization–delocalization transition on thermoelectric properties of Bi₂Te₂Se topological insulator. *APL Energy*, 2(1).
9. Gong, Y., Chang, C., Wei, W., Liu, J., Xiong, W. et al. (2018). Extremely low thermal conductivity and enhanced thermoelectric performance of polycrystalline SnSe by Cu doping. *Scripta Materialia*, 147, 74-78.
10. Ding, G., Gao, G., & Yao, K. (2015). High-efficient thermoelectric materials: The case of orthorhombic IV-VI compounds. *Scientific reports*, 5(1), 9567.
11. Gainza, J., Serrano-Sanchez, F., Rodrigues, J. E., Huttel, Y., Dura, O. J. et al. (2020). High-performance n-type SnSe thermoelectric polycrystal prepared by arc-melting. *Cell Reports Physical Science*, 1(12).
12. Guan, X., & Ouyang, J. (2021). Enhancement of the Seebeck coefficient of organic thermoelectric materials via energy filtering of charge carriers. *CCS Chemistry*, 3(10), 2415-2427.
13. Guttmann, G. M., Gertner, R., Samuha, S., Ben-Ayoun, D., Haroush, S. et al. (2018). Thermoelectric and mechanical properties of Ag and Cu doped (GeTe)_{0.96}(Bi₂Te₃)_{0.04}. *MRS Communications*, 8(3), 1292-1299.
14. Haupt, S., Edler, F., Bartel, M., & Pernau, H. F. (2020). Van der Pauw device used to investigate the thermoelectric power factor. *Review of Scientific Instruments*, 91(11).
15. Huang, Z., Dai, X., Yu, Y., Zhou, C., & Zu, F. (2016). Enhanced thermoelectric properties of p-type Bi_{0.5}Sb_{1.5}Te₃ bulk alloys by electroless plating with Cu and annealing. *Scripta Materialia*, 118, 19-23.
16. Jia, S. Z. (2023). Waste energy harvesting in sustainable manufacturing. *In Sustainable Manufacturing Processes* (pp. 231-256). Academic Press.
17. Justl, A. P., Ricci, F., Pike, A., Cerretti, G., Bux, S. K. et al. (2022). Unlocking the thermoelectric potential of the Ca₁₄AlSb₁₁ structure type. *Science Advances*, 8(36), eabq3780.
18. Karpov, A. V., Sytshev, A. E., & Sivakova, A. O. (2023). Device for measurement the seebeck coefficient of thermoelectric materials in the temperature range 300–800 K. *Measurement Techniques*, 66(8), 628-635.
19. Kockert, M., Kojda, D., Mitdank, R., Mogilatenko, A., Wang, Z. et al. (2019). Nanometrology: Absolute Seebeck coefficient of individual silver nanowires. *Scientific reports*, 9(1), 20265.
20. Lowhorn, N. D., Wong-Ng, W., Lu, Z. Q., Thomas, E., Otani, M. et al. (2009). Development of a seebeck coefficient standard reference material. *Applied Physics A*, 96, 511-514.
21. Liu, Z. K. (2022). Theory of cross phenomena and their coefficients beyond Onsager theorem. *Materials Research Letters*, 10(7), 393-439.
22. Pallechi, I., Buscaglia, M. T., Buscaglia, V., Gilioli, E., Lamura, G. et al. (2016). Thermoelectric behavior of Ruddlesden-Popper series iridates. *Journal of Physics: Condensed Matter*, 28(6), 065601.
23. Pokharel, M., Zhao, H., Lukas, K., Ren, Z., Opeil, C. et al. (2013). Phonon drag effect in nanocomposite FeSb₂. *MRS Communications*, 3, 31-36.
24. Ramachandran, B., Wu, K. K., Kuo, Y. K., Guo, L. S., & Wang, L. M. (2016). Compositional effects on the low-temperature transport properties of non-stoichiometric Bi₂TexSey-based crystals. *Journal of Physics D: Applied Physics*, 50(2), 025302.
25. Schrade, M., Fjeld, H., Norby, T., & Finstad, T. G. (2014). Versatile apparatus for thermoelectric characterization of oxides at high temperatures. *Review of Scientific Instruments*, 85(10).
26. Secco, R. A. (2017). Thermal conductivity and Seebeck coefficient of Fe and Fe-Si alloys: Implications for variable Lorenz number. *Physics of the Earth and Planetary Interiors*, 265, 23-34.
27. Snyder, G. J., Pereyra, A., & Gurunathan, R. (2022). Effective mass from seebeck coefficient. *Advanced Functional Materials*, 32(20), 2112772.
28. Snyder GJ, Snyder AH, Wood M et al. 2020. Weighted mobility. *Advanced Materials* 32: 2001537.

29. Zhou, C., Lee, Y. K., Yu, Y., Byun, S., Luo, Z. Z. et al. (2021). Polycrystalline SnSe with a thermoelectric figure of merit greater than the single crystal. *Nature materials*, 20(10), 1378-1384.
30. Zhang, Z., Yan, Y., Li, X., Wang, X., Li, J. et al. (2020). A dual role by incorporation of magnesium in YbZn₂Sb₂ Zintl phase for enhanced thermoelectric performance. *Advanced Energy Materials*, 10(29), 2001229.
31. Wu, L., Li, X., Wang, S., Zhang, T., Yang, J. et al. (2017). Resonant level-induced high thermoelectric response in indium-doped GeTe. *NPG Asia Materials*, 9(1), e343-e343.